Int.J.Curr.Microbiol.App.Sci (2025) *14*(02): 206-216

International Journal of Current Microbiology and Applied Sciences
***ISSN: 2319-7706* Volume 14 Number 2 (2025)**
Journal homepage: http://www.ijcmas.com

Original Research Article https://doi.org/10.20546/ijcmas.2025.1402.019

Evaluation of *In-Vitro* and *In-Silico* Study of Anti-Tubercular Activity in *Senna sophera* Seeds

K. V. Vinothini[1*], K. Vijay Krishnan[1], S. Shervinjose[2], K. Kanimozhi[3], T. B. Taanika[2] and T. Siva Nandhini[2]

[1]Department of Pharmacology, Ultra College of Pharmacy, Madurai, Tamil Nadu, India
[2]S A Raja Pharmacy College, Vadakkankulam, Tirunelveli District, Tamil Nadu, India
[3]Department of Pharmaceutics, Ultra College of Pharmacy, Madurai, Tamil Nadu, India

**Corresponding author*

Keywords

Senna sophera, tuberculosis, Broth Microdilution Method, H37Rv, Molecular docking, Molecular dynamic

Article Info

Received:
15 December 2024
Accepted:
29 January 2025
Available Online:
10 February 2025

A B S T R A C T

Tuberculosis (TB) is a serious health issue worldwide. TB continues to be the most common infectious agent-related cause of mortality worldwide. A yield of 5.25%w/w was obtained from the methanolic extract of *Senna sophera* seeds. Alkaloids, carbohydrates, saponins, phenolic substances, flavonoids, terpenoids, glycosides, and steroids were included in the initial phytochemical analysis of *the Senna sophera* seed extract in methanol. Compared to the relative concentration of Rifampicin, the Broth Microdilution Method, which was used to examine the anti-tubercular activity of *Senna sophera* seeds against H37Rv, revealed a moderate inhibition of growth with an MIC of 500 µg/ml. Based on ADME and toxicity prediction, GC-MS analysis of *Senna sophera* seed extract showed that this plant is a rich source of phytoconstituents with a high binding affinity in docking experiments and compounds with drug-like features. This study used AutoDock Vina molecular docking simulations to evaluate the binding interactions between various ligands and a target protein model. Docking scores and 2D interaction images were made accessible for visualization. The data showed that 5UHB-DRG2 had the best docking score of -6.7, indicating a stronger binding affinity due to interactions with crucial residues such as GLN C:438 and LEU C:436. However, additional ligands, including 5UHB-DRG1 and 5UHB-DRG3, had scores of -4.7 and -4.8, respectively, while 5UHB-DRG4 and 5UHB-DRG5 also received -4.1. Furthermore, as indicated by its score of -4.1, the 5UHB-RIF complex exhibited competitive binding properties with lower-scoring DRG complexes.

Introduction

Tuberculosis (TB) is an airborne infectious illness caused by bacteria from the *Mycobacterium tuberculosis* complex. *M. tuberculosis* is primarily a lung infection, but it can infect practically any area of the body. Infection with *M. tuberculosis* can progress from containment in the host, in which the bacteria are isolated

within granulomas (latent TB infection), to a contagious condition, in which the patient exhibits symptoms such as cough, fever, night sweats, and loss of weight. Only active tuberculosis is communicable (WHO, 2015). From a clinical and public health standpoint, patients with tuberculosis are pragmatically classified as having latent tuberculosis infection (LTBI), which is an asymptomatic and non-transmissible state, or active tuberculosis disease, which is transmissible (in active pulmonary tuberculosis) and can be diagnosed using culture-based or molecular tests. Patients with active tuberculosis have general symptoms such as fever, weariness, loss of appetite, and weight loss, while those with pulmonary illness may have a chronic cough and hemoptysis (coughing up blood) in advanced disease. However, some patients with active, culture-positive illness may be asymptomatic, indicating silent tuberculosis (Barry *et al.,* 2009; Esmail *et al.,* 2014).

Seennasophera, also known as 'Kasondi', is a significant medicament in the Islamic System of Medicine. According to Unani literature, 'Kasondi' is repulsive of morbid humours (particularly phlegm), resolvent, blood purifier, carminative, purgative, digestive, and diaphoretic, and has been used to treat epilepsy, ascites, liver dyscrasia, skin disorders, piles, jaundice, fever, articular pain, and palpitation. According to ethnobotanical literature, it is beneficial in the treatment of pityriasis, psoriasis, asthma, acute bronchitis, cough, diabetes, and children's convulsions. *Senna sophera* seeds contain ascorbic acid, dehydroascorbic acid, and β-sitosterol, but no scientific studies have been conducted on the plant's varietal level. The plants contain a wide range of secondary metabolites, including steroids, glycosides, terpenoids, alkaloids, and flavonoids, all of which have been shown to have antimicrobial activities (The Ayurvedic Pharmacopoeia of India; Agarwal and Paridhavi, 2005; Meena and Kalidhar, 1998).

Materials and Methods

Place of study

Anti-tubercular activity and micro-broth dilution assays were performed at the ICMR-National Institute for Research in Tuberculosis, Chetpet, Chennai- 600031.GC-MS Analysis was carried out at the Royal Bio Research Centre, Velachery, Chennai-600042.An in silico study was carried out by Scioimics in Ooty, Tamil Nadu.

Collection of Plants

The seeds of *Senna sophera* were collected from Madurai and authenticated by Dr. D. Stephen Ph.D., Lecturer, Department of Botany, The American College, Madurai 02.

Preparation of Extract

Senna sophera seeds were collected, shade-dried at room temperature, and coarsely ground using a dry grinder. About 180g of coarse powder of seed of *Senna sophera* was packed in the Soxhlet apparatus directly with 500 ml of methanol. The methanolic extract was evaporated at 60^0C using a rotary evaporator. The extracted material was stored in an airtight container for later investigation (López-Bascón and De Castro, 2020).

Qualitative phytochemical analysis

Ethanol extract are tested for the presence of various active phytoconstituents namely steroids, alkaloids, tannins, phenolic compounds, flavonoids, diterpenes, triterpenes and saponins.

Evaluation of Anti-Tubercular Activity

Determination of minimum inhibitory concentration by broth dilution method

The crude extract was initially screened using the wild-type H37Rv. Multidrug-resistant (MDR) Mycobacterium TB clinical isolates and susceptible strains (stored clinical isolates from the National Institute for Research in TB). A smooth suspension of H37Rv was extracted from 3 weeks old LJ medium and placed in a biju bottle containing glass beads in Middlebrook 7H9 medium supplemented with OADC (10% v/v) (oleic acid, albumin, dextrose, and catalase) and glycerol (0.2%). To prevent clumping, the suspension was vortexed rapidly for 30 s and adjusted to 1 McFarlan standard (3 × 106 CFU/mL).

The inoculum was diluted further in 7H9 media to generate a 1:20 dilution (0.5 ml of the suspended strain in 9.5 ml of 7H9 media. In a 96-well plate with a flat bottom, 100µl of OADC and 0.5% glycerol-enriched 7H9 were added along with 100µl of extracts at various concentrations that were serially diluted (2-fold). In each well, 100µl of bacterial inoculum (1:20) was added and

cultured for 7–14 days for H37Rv and 7–21 days for the clinical isolates at 37°C and 5% CO2. Following incubation, the plates were examined under a microscope to determine gradation based on the serpentine chord formation of Mtb culture growth. All tests were carried out in duplicate in a microtiter plate, and the MIC was defined as the plant extract concentration that completely or 90% suppressed Mtb growth (Mann and Markham, 1998).

GC-MS Analysis

The GC-MS analysis of *Senna sophera* seeds was performed on an Agilent 7890A system equipped with a mass spectrophotometer detector and a splitless injection mechanism. The GC used an HP-5MS capillary column (30m× 0.25 mm) with a film thickness of 0.25 µm. The temperature program was as follows. Injector temperature: 260°C; starting oven temperature: 70°C; then increased at 10°C/min to 150°C for 5 minutes; 12°C/min to 200°C for 15 minutes; and 12°C/min to 220°C for 15 minutes. Helium was employed as the carrier gas at a pressure of 17.69 psi and a flow rate of 0.6ml/min. Samples were dissolved in methanol, and a 1 µl aliquot was automatically injected. MS was set to scan mode. The mass range was chosen between 50 and 550m/z. MS spectra of separated components were detected using NIST library data (Kumar and Pandey, 2013).

Molecular Docking

In this study, ligands against the crystal structure of *Mycobacterium tuberculosis* transcription initiation complex in association with Rifampin (5UHB) were molecularly docked using AutoDock Vina. Following their collection from Pubchem, the 3D structures of the ligands were initially prepared for docking using the Open Babel tool.

Docking preparations were also performed for the receptor, which is the crystal structure of *Mycobacterium tuberculosis* transcription initiation complex in association with Rifampin (5UHB). The AutoDock Vina docking technique was configured with the search space and grid box size of 60 x 60 x 60. Additionally, docking runs for triple docking were initiated. The binding affinities of the resulting docking positions were investigated, and the optimum poses were selected for further study. PyMOL software was used to study ligand-receptor interactions and binding modes. The docking study data was used to evaluate the potential of medicines and phytochemicals as inhibitors of the crystal structure of the *Mycobacterium tuberculosis* transcription initiation complex in association with Rifampin (5UHB) (Lipinski *et al.,* 2012).

Molecular dynamics

The structure of *Mycobacterium tuberculosis* transcription initiation complex in complex with Rifampin (5UHB) was crystallized. The top ligands identified from docking analysis, such as Drug (DRG) and Rifampin (RIF), were chosen from the ATB server. The ligand topology was chosen from the ATB server, and the pdb2gmx, a module of GROMACS, was used to add hydrogens to the heavy atoms. The prepared systems were first vacuum minimized for 1500 steps using the steepest descent algorithm, and then the structures were solvated in a cubic periodic box. The complex systems were then maintained at a salt concentration of 0.15 M by adding appropriate amounts of Na and Cl counter ions. The system preparation was based on a previously published study. Each structure that emerged from the NPT equilibration phase was exposed to a final production run in the NPT ensemble for 100 ns of simulation time. Finally, the simulation trajectory was analyzed using the Gromacs software package's various tools, which included the protein root mean square deviation (RMSD), root mean square fluctuation (RMSF), radius of gyration (RG), solvent accessible surface area (SASA), hydrogen bonding (H-Bond), Principal Component Analysis (PCA), and Free Energy Landscape (FEL). The Molecular Mechanics Poisson-Boltzmann surface area (MM-PBSA) approach was used to determine the binding free energy (5UHB-DRG, RIF binding) of an inhibitor with protein across simulation time. A GROMACS function gmmpbsa was used to calculate the binding free energy. To get an accurate result, we computed 5UHB-DRG and 5UHB-RIF for the latest 50 ns with dt = 1000 frames (Zeb *et al.,* 2021; Anandakrishnan *et al.,* 2012; Berendsen *et al.,* 1995; Brooks *et al.,* 1983; Jurcik *et al.,* 2018).

Results and Discussion

Phytochemical analysis

The result shows the preliminary phytochemicals: tannins, terpenes, phenols, steroids, saponins, alkaloids, flavonoids, and glycosides. It is an important and rich source of secondary metabolites.

Micro Dilution Broth Assay

The antitubercular potency of a methanolic extract of *Senna sophera* seeds was assessed using the Micro Broth Dilution Method. After 14 days of incubation at 37°C, the growth and inhibition of *M. tuberculosis* H37Rv, a monoresistant isolate, were measured in extract-containing and extract-free control wells. *Senna sophera* seed extract shown activity against tested strains in broth dilution experiments, with a MIC of 500µg/mL.

GC-MS Analysis

The GC-MS study of *senna sophera* seed extract demonstrated that this plant is a rich source of phytoconstituents which is show in given table no 2

ADME Analysis for the GC-MS compounds

The ADME attributes of GC-MS compounds were investigated further using the web programs Swiss ADME and ADME calculator to determine their pharmacokinetics, drug-likeness, and physiochemical features. Palmitic acid, oleic acid, linoleic acid, and beta-sitosterol all comply with Lipinski's rule of five. According to Lipinski's rule, practically all of the GC-MS compounds exhibited orally active drug-like characteristics. Compounds with low lipophilicity, molecular weight, and hydrogen bond capacity are thought to have high permeability, absorption, and bioavailability.

Molecular Docking of GC-MS compounds

The protein model was tested to molecular docking with Autodock vina. The docking scores of the chosen ligands docked with the target proteins were tabulated.

Molecular Dynamics

All-atom MD simulation is an appropriate technique for studying the structural dynamics of proteins and how they interact with ligands. Due to its ability to analyze chemical systems in great detail at the atomic level, this approach has completely changed the field of computer-aided drug design and discovery. The dynamic alterations that take place when the target protein binds were examined in this study using MD simulations. Numerous metrics, including intermolecular hydrogen bonding, Rg, SASA, RMSD, and RMSF, were computed for the protein and protein-ligand complex. Principal component analysis and free energy landscapes were also examined during the simulation's 100 ns trajectory.

Root Mean Square Deviation (RMSD)

The RMSD readings were examined over time to look at the stability of the 5UHB complex and learn more about the systems' behavior. The findings show that both systems were evenly dispersed throughout the simulation and reached equilibrium after 20 ns. APO, DRG, and RIF were shown to have average RMSD values of 0.83 +/- 0.11 nm, 0.96 +/- 0.14 nm, and 1.07 +/- 0.12 nm, respectively. Additionally, the evaluation of the RMSD values showed that the docked complex remained stable throughout the simulation, with the APO, DRG, and RIF maintaining stability for up to 100 ns. According to this result, the APO, DRG, and RIF system is stable and did not show any notable oscillations throughout the experiment.

Root Mean Square Fluctuation (RMSF)

To measure the changes of each residue and flexible region of a protein, MD simulations employ RMSF. By looking at RMSF during simulations, one can determine how ligand binding affects the protein. RMSF values are generally higher for loosely arranged loop segments than for compact protein structures such as helices and sheets. The RMSF values for each complex were calculated and displayed in this study for every residue in the DRG and RIF complex (as shown in Figure 2). The average RMSF values for APO, DRG, and RIF were found to be 0.30 +/- 0.16 nm, 0.27 +/- 0.15 nm, and 0.32 +/- 0.21 nm, respectively. The results demonstrate that the combination of DRG and RIF did not significantly alter the overall RMSF distribution.

Radius of gyration (Rg)

The Rg values were calculated and plotted over time to evaluate the dynamic stability and compactness of APO and its complex 3.51 +/- 0.03 nm, 3.50 +/- 0.04 nm, and 3.60 +/- 0.04 nm were found to be the average Rg values for DRG and RIF, respectively. The DRG complex system was marginally more compact than the RIF complex system, as seen by the Rg values being significantly lower.

Solvent accessible surface area (SASA)

SASA is a useful metric for evaluating the accessibility of a protein molecule in a solvent environment. In this study, the impact of DRG and RIF complexes on the

solvent accessibility of the target was determined using the computation and visualization of SASA values.

A similar pattern can be seen in the plot of the DRG SASA values following binding with RIF. An average SASA value of 549.25 +/- 10.2 nm was found for DRG, 544.74 +/- 15.5 nm for RIF, and 546.55 +/- 16.6 nm for RIF. The SASA values show fair equilibration throughout the experiment, with no discernible changes.

Intra and Inter Hydrogen Bond

To assess the stability of Protein alone (APO) and Protein-ligand (DRG and RIF) interactions, the formation of Intra and Inter Hydrogen Bond plays a crucial role. In this study, we investigated the time-dependent behavior of Intra hydrogen bonds DRG and RIF complexes and plotted the results (Figure 5). The average Intra H-Bond values for DRG and RIF Complex were determined to be 845.23 +/- 15.6 nm, 844.93 +/- 17.03 nm and 848.84 +/- 19.7 nm, respectively.

To assess the stability of protein-ligand interactions, the formation of hydrogen bonds plays a crucial role. In this study, we investigated the time-dependent behavior of hydrogen bonds between DRG and RIF and plotted the results (Figure 6).

The plot revealed that despite higher fluctuations, up to four hydrogen bonds were formed between DRG and RIF. Our analysis indicates that the docked complex remained stable during the simulation, maintained by at least 1 to 6 hydrogen bonds with DRG and 1 to 3 with RIF.

Principal Component Analysis (PCA)

We used PCA to investigate the collective movements in DRG and RIF. The global motion of a protein molecule is significantly influenced by the first few eigenvectors (EVs). In order to investigate the structural dynamics of DRG and RIF during the simulation, we performed PCA (Figure 7). According to PCA's time evolution, both EVs' total DRG and RIF complex flexibility decreased, suggesting stability (Figure 7).

The plot unequivocally shows that the DRG and RIF complex overlapped and occupied nearly all of the conformational movements. Generally speaking, the smaller number of movements seen in the RIF indicates that the target conformation and dynamics were not substantially impacted by the RIF, hence confirming the complex's stability.

Free Energy Landscapes (FELs)

Free energy landscape (FEL) analysis is a popular method for examining the general stability and processes of protein folding. The most stable conformational ensembles for a protein structure are shown by FEL plots. Here, we created FEL plots for PC1 and PC2, where darker blue patches show lower energy and more stable protein conformations. Throughout the DRG and RIF simulations, the plots show energy values ranging from 0 to 16 kJ/mol and 0 to 20 kJ/mol, respectively. The DRG and RIF complex exhibits a single global minimum that is contained within a sizable local basin, according to the FEL plots. These results imply that the target structure is stabilized by DRG and RIF as they do not significantly alter its conformation (Figure 8).

Table.1 MIC of Plant extract against the microorganism by micro dilution broth assay

Sample	Concentration	MIC (µg/ml)
		H37RV
Senna sophera	1000 500 250 125 62.5 31.25 15.6 7.8	500 µg/ml
Rifampicin	Critical concentration	1 µg/ml

Table.2 GC-MS Analysis of methanolic extract of *Senna sophera*

Peak#	R.Time	Area	Area %	Height	Name
1	25.215	18018	0.01	5736	**bicyclo[4.1.0]heptan-3-ol,4,7,7-trimethyl-, (1.alpha.,3.beta.,**
2	25.387	17715087	6.82	4703256	**carbonicacid,(1r)-(-)-menthyloctylester**
3	25.595	191626	0.07	33423	**n-pentadecanol**
4	25.750	1133364	0.44	182901	**9,12-octadecadienoicacid,methylester**
5	25.994	49128	0.02	14386	**isophytol,acetate**
6	26.113	27610	0.01	10034	**octadecanoicacid,methylester**
7	26.331	30324675	11.67	3087594	**cis-9-hexadecenal**
8	26.591	11371439	4.38	700552	**octadecanoicacid**
9	27.380	808389	0.31	80706	**carbonicacid,but-2-yn-1-ylundecylester**
10	27.570	353336	0.14	52300	**9-octadecene,1-(2,3-dimethoxypropoxy)-,(z)-(.+-.)-**
11	27.681	324056	0.12	39814	**2,2-dideuteroheptadecanal**
12	27.860	103802	0.04	20567	**2-(dimethylamino)ethyl1-adamantanecarboxylate**
13	28.068	4320600	1.66	949058	**octanoicacid,2-dimethylaminoethyl ester**
14	28.233	508412	0.20	96063	**Triarachine**
15	28.491	7104359	2.73	821899	**decanamide,n-(2-hydroxyethyl)-**
16	28.820	513559	0.20	68431	**dodecanamide,n-(2-hydroxyethyl)-**
17	29.010	92620	0.04	18847	**2(3h)-thiazolethione,dihydro-4-(hydroxyamino)-5,5-dimethyl-3-(1-methyleth**
18	29.483	220611	0.08	34066	**undec-10-ynoicacid,undec-2-en-1-ylester**
19	29.660	114950	0.04	24784	**dodecahydro-6h-pyrido[1,2-b]isoquinolin-6-one**
20	29.734	200177	0.08	32248	**(r)-(-)-14-methyl-8-hexadecyn-1-ol**
21	29.910	7738	0.00	1876	**benzamide,n-[(ethylamino)carbonyl]-**
22	30.069	14887837	5.73	2577427	**3-cyclopentylpropionicacid,2-dimethylaminoethyl ester**
23	30.275	1262361	0.49	251064	**oleic acid**
24	30.360	1052873	0.41	186909	**3-cyclopentylpropionicacid,2-dimethylaminoethyl ester**
25	30.528	1175234	0.45	115527	**1h-indene,2,3-dihydro-1-methyl-**
26	30.718	4949316	1.90	447375	**palmitic acid**
27	31.149	1392618	0.54	161502	**benzyldiethyl-(2,6-xylylcarbamoylmethyl)-ammoniumbenzoate**
28	31.330	152762	0.06	34318	**6-[1-naphthylacetyl]-2,4-diamino-6,7-dihydro-5h-pyrrolo[3,4-d]pyrimidine**
29	31.493	229249	0.09	30645	**heptadecane,8-methyl-**
30	31.683	212525	0.08	22410	**5-bromo-1h-1,2,3-triazole-4-carboxylicacid**
31	31.782	122980	0.05	20490	**methyl2-bromodecanoate**
32	31.923	39340	0.02	9230	**6-methyl-5-[1-piperidinyl]-2,4-pyrimidinediamine**
33	32.075	12784	0.00	1300	**beta –sitosterol**
34	32.199	291923	0.11	61245	**1,1-dichloro-2,2,3,3-tetramethylcyclopropane#**
35	32.393	1098883	0.42	147368	**14-methyl-8-hexadecyn-1-ol#**
36	32.572	54976	0.02	14055	**ascorbic acid 2,6-dihexadecanoate**
37	**32.701**	**9343899**	**3.60**	**1006627**	**linoleic acid, 9,cis-12-octadecadienoic acid**

Table.3 ADME property prediction for the GC-MS compounds

S. No	Compounds	Molecular weight	HB Acceptor	HB Donor	Liphophilicity	Molar Refractivity	Rule of five	GI Absorption
1	Palmictic acid	256.42	2	1	5.20	80.80	1	HIGH
2	Oleic acid	282.46	2	1	5.65	89.94	1	HIGH
3	Linoleic acid	280.24S	2	1	4.597	89.46	1	LOW
4	Beta-sitosterol	414.71	1	1	7.24	133.23	1	LOW
5	Ascorbic acid	176.12	6	4	-1.42	35.12	0	HIGH

Table.4 Docking scores and interactions with the protein

Protein-Ligand Complex	Docking score	Interactions
5UHB-PALMITIC ACID	-4.7	ARG C:454, GLN C:438, LEU C:436, VAL C:176, SER C:456, ILE C:497, LEU C:458, GLN C:435
5UHB-OLEIC ACID	-6.7	GLN C:438, LEU C:436, SER C:437, LEU C:458, GLN C:435, SER C:456, ILE C:497, PHE C:439, ARG C:465, GLY C:459
5UHB-LINOLEIC ACID	-4.8	GLN C:435, LEU C:458, ARG C:465, SER C:437, GLY C:459, GLN C:439, ILE C:497, ASN C:489, GLY C:491, PRO C:492, GLN C:614
5UHB-BETA –SITO STEROL	-4.1	ASN C:611, GLU C:487, THR C:488, GLY C:491, ARG C:454, THR C:450, ILE C:497, ASN C:610, PRO C:489, GLN C:619
5UHB-ASCORBIC ACID	-4.1	ASN C:610, GLN C:614, PRO C:492, ARG C:454, GLY C:491, GLU C:487, THR C:488, ILE C:497, THR C:450

Table.5 Binding strength of DRG and RIF

System	van der Waal energy (kJ/mol)	Electrostatic energy (kJ/mol)	Polar solvation energy (kJ/mol)	Binding energy (kJ/mol)
DRG	-261.965 ± 9.051	-8.021 ± 3.147	122.343 ± 11.280	-173.549 ± 9.175
RIF	-255.135 ± 19.930	-30.884 ± 10.923	169.317 ± 17.801	-143.636 ± 13.362

Figure.1 RMSD Conformational dynamics analysis of APO, DRG and RIF

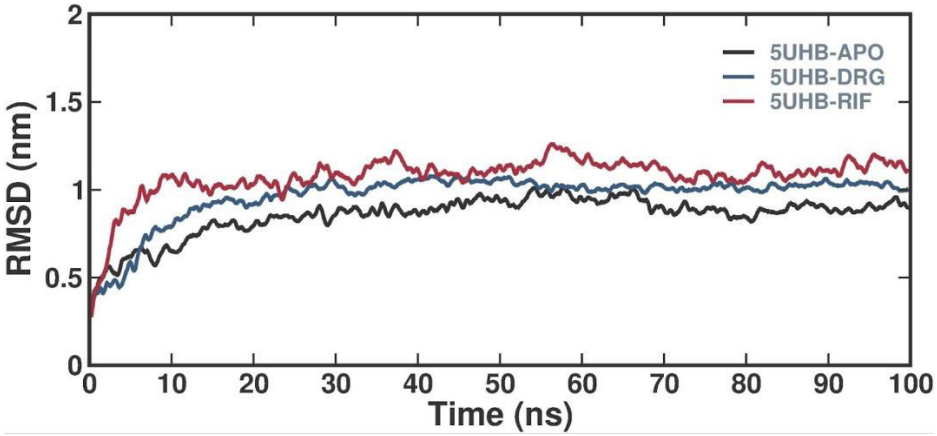

Figure.2 RMSF Conformational dynamics analysis of APO, DRG and RIF complex.

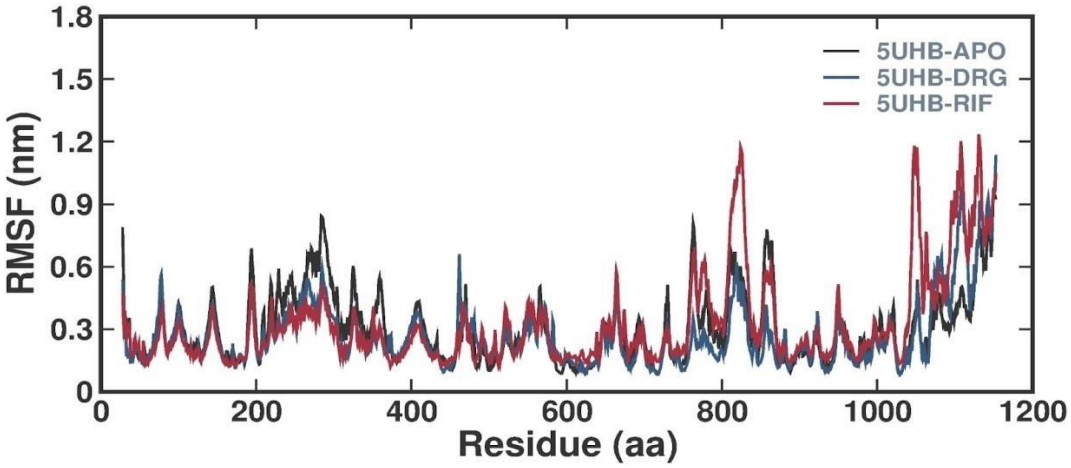

Figure.3 Rg Conformational dynamics analysis of APO, DRG and RIF complex.

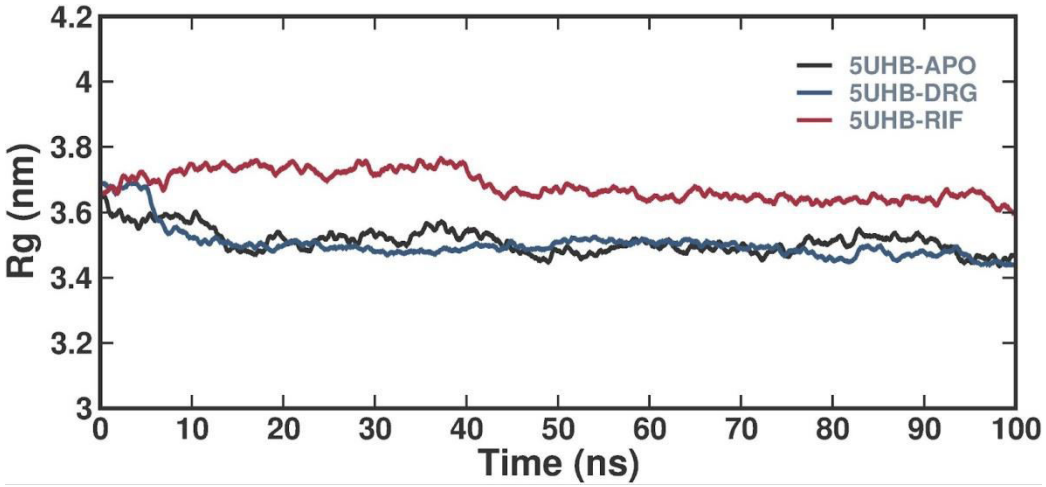

Figure.4 SASA Conformational dynamics analysis of APO, DRG and RIF complex

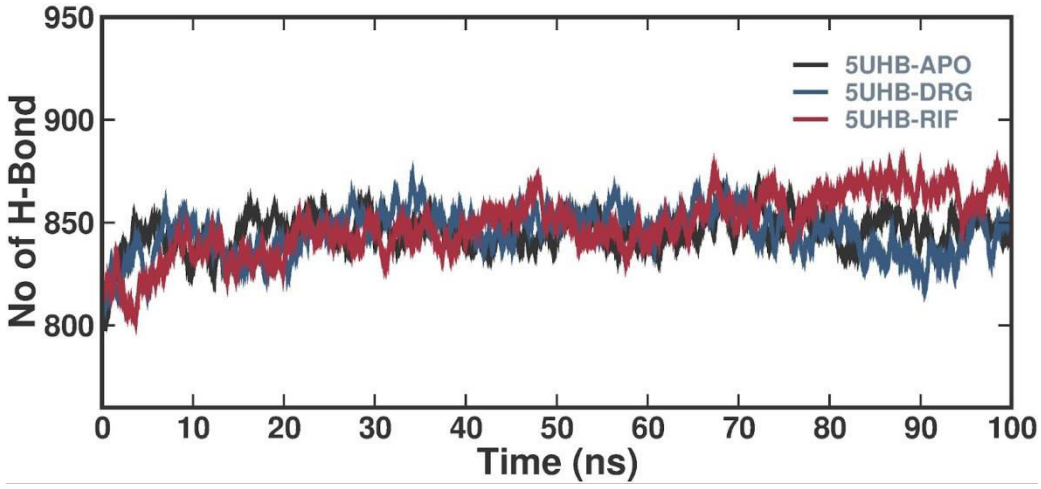

Figure.5 Intramolecular hydrogen bonds APO, DRG and RIF during the simulation time.

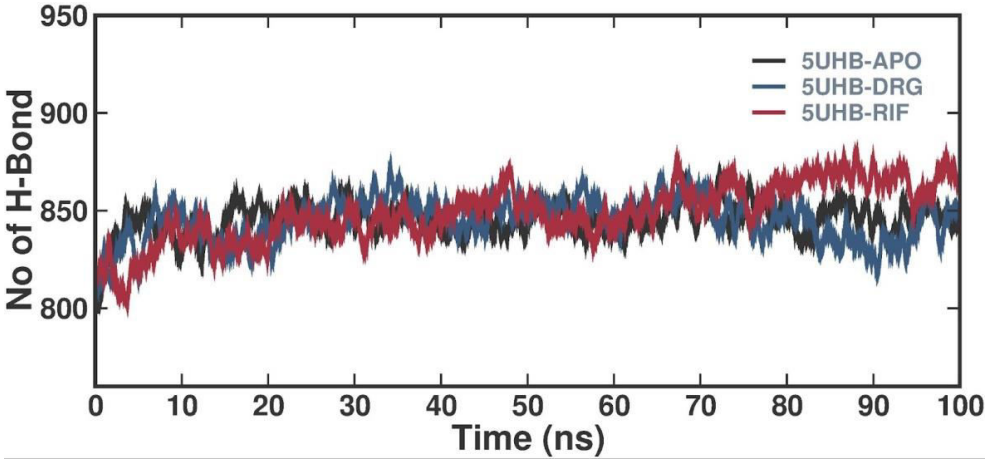

Figure.6 Intermolecular hydrogen bonds DRG and RIF during the simulation time.

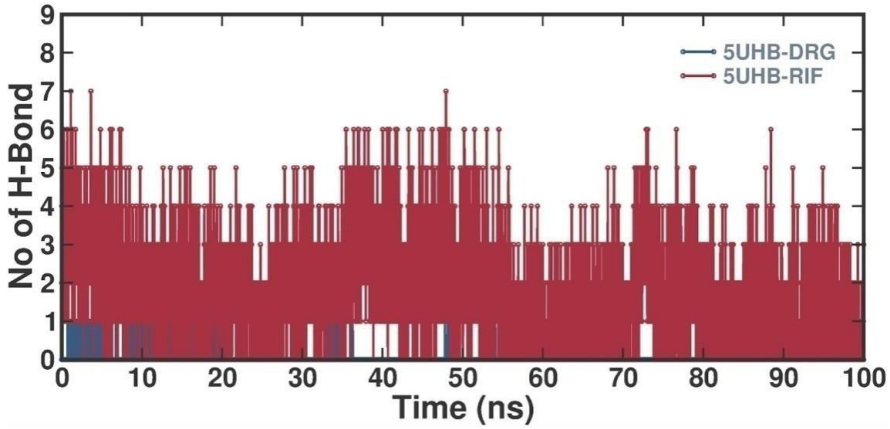

Figure.7 Principal Component analysis 2D projection plot shows the conformation sampling of APO, DRG and RIF on PC1 and PC2.

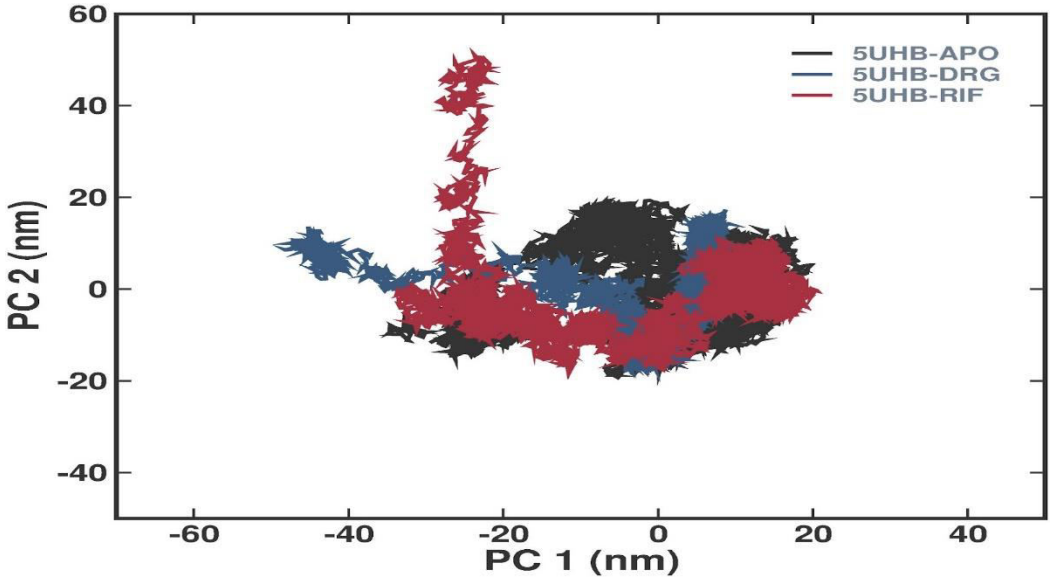

Figure.8 The free energy landscape plots for (A) APO (B) DRG (C)RIF Complex.

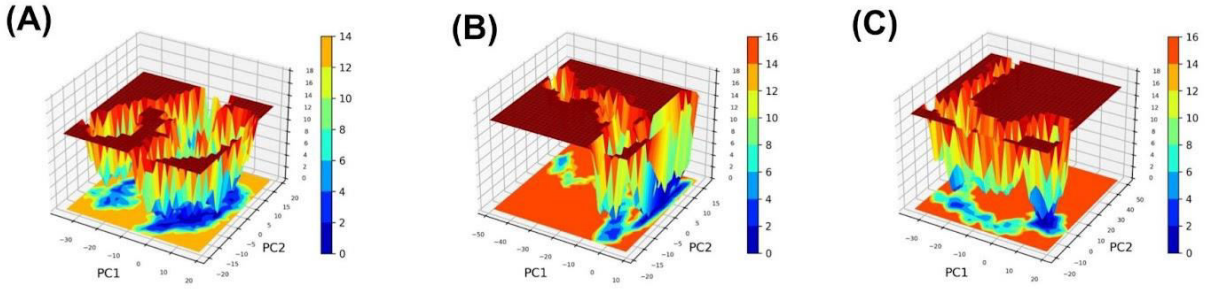

This study used AutoDock Vina molecular docking simulations to evaluate the binding interactions between various ligands and the target protein model. For visualization, docking scores and 2D interaction images were made accessible.

The data showed that 5UHB-DRG2 had the best docking score of -6.7, indicating a stronger binding affinity due to interactions with crucial residues such as GLN C:438 and LEU C:436.

However, additional ligands, including 5UHB-DRG1 and 5UHB-DRG3, had scores of -4.7 and -4.8, respectively, while 5UHB-DRG4 and 5UHB-DRG5 also received -4.1. Furthermore, as indicated by its score of -4.1, the 5UHB-RIF complex exhibited competitive binding properties with the lower-scoring DRG complexes. These results highlight the different DRG ligand binding affinities and imply that particular residues are essential for maintaining ligand binding, laying the groundwork for additional research into their biochemical significance and possible therapeutic uses.

Acknowledgement

Department of Pharmacology, Ultra College of Pharmacy, Madurai.

Funding Source

Nil.

Author Contributions

K. V. Vinothini: Investigation, formal analysis, writing—original draft. K. Vijay Krishnan: Validation, methodology, writing—reviewing. S. Shervinjose:—Formal analysis, writing—review and editing. Kanimozhi: Investigation, writing—reviewing. T. B. Taanika: Resources, investigation writing—reviewing. T. Nandhini: Validation, formal analysis, writing—reviewing.

Data Availability

The datasets generated during and/or analyzed during the current study are available from the corresponding author on reasonable request.

Declarations

Ethical Approval Not applicable.

Consent to Participate Not applicable.

Consent to Publish Not applicable.

Conflict of Interest The authors declare no competing interests.

References

Agarwal SS and Paridhavi M. Clinically useful herbal drugs. 2005;281-282.

Anandakrishnan, R., Aguilar, B., &Onufriev, A. V. (2012). H++ 3.0: automating pK prediction and the preparation of biomolecular structures for atomistic molecular modeling and simulations. [Research Support, N.I.H., Extramural]. *Nucleic Acids Res, 40* (Web Server issue), pp. W537-541. https://doi.org/10.1093/nar/gks375

Barry, C. E. 3rd *et al.,* The spectrum of latent tuberculosis: rethinking the biology and intervention strategies. *Nat. Rev. Microbiol.* 7, 845–855 (2009).

Berendsen, H. J., van der Spoel, D., & van Drunen, R. (1995). GROMACS: a message-passing parallel molecular dynamics implementation. *Computer physics communications.* 43-56 https://doi.org/10.1016/0010-4655(95)00042-E

Brooks, B. R., Bruccoleri, R. E., Olafson, B. D., States, D. J., Swaminathan, S. a., & Karplus, M. (1983). CHARMM: a program for macromolecular energy, minimization, and dynamics calculations. *J Comput Chem.* 187-217 https://doi.org/10.1002/jcc.540040211

Esmail, H., Barry, C. E. 3rd, Young, D. B. & Wilkinson, R. J. The ongoing challenge of latent tuberculosis. *Phil. Trans. R. Soc. B* 369, 20130437 (2014). https://doi.org/10.1098/rstb.2013.0437

Jurcik, A., Bednar, D., Byska, J., Marques, S. M., Furmanova, K., Daniel, L., Kokkonen, P., Brezovsky, J., Strnad, O., Stourac, J., Pavelka, A., Manak, M., Damborsky, J., &Kozlikova, B. (2018). CAVER Analyst 2.0: analysis and visualization of channels and tunnels in protein structures and molecular dynamics trajectories 3586-3588. https://doi.org/10.1093/bioinformatics/bty386

Kumar S, Pandey AK. Chemistry and biological activities of flavonoids: an overview. Scientific World Journal. 2013, 162750. https://doi.org/10.1155/2013/162750

Lipinski, C.A.; Lombardo, F.; Dominy, B.W.; Feeney, P.J. In Vitro models for selection of development candidates experimental and computational approaches to estimate solubility and permeability in drug discovery and development settings. Adv. Drug Deliv. Rev. 2012, 23,3–25.

López-Bascón, M.A. and De Castro, M.L., 2020. Soxhlet extraction. In Liquid-phase extraction (pp. 327-354). Elsevier. https://doi.org/10.1016/B978-0-12-816911-7.00011-6

Mann, C. M. & Markham, J. L. (1998). A new method for determining the minimum inhibitory concentration of essential oils. 538-44. https://doi.org/10.1046/j.1365-2672.1998.00379.x

Meena R and Kalidhar SB. Organic including Medicinal plants. Indian Journal of Chemistry. 1998; 37(12):1314-1315

The Ayurvedic Pharmacopoeia of India.

World Health Organization. *Global Tuberculosis Report 2015* (WHO, 2015)

Zeb, M.A., Rahman, T.U., Sajid, M., Xiao, W., Musharraf, S.G., Bibi, S., Akitsu, T. and Liaqat, W., 2021. GC-MS analysis and in silico approaches of *Indigo feraheterantha* root oil chemical constituents. *Compounds*, *1*(3), pp.116-124. http://dx.doi.org/10.3390/compounds1030010

How to cite this article:

Vinothini, K. V., K. Vijay Krishnan, S. Shervinjose, K. Kanimozhi, T. B. Taanika and Siva Nandhini, T. 2025. Evaluation of *In-Vitro* and *In-Silico* Study of Anti-Tubercular Activity in *Senna sophera* Seeds. *Int.J.Curr.Microbiol.App.Sci.* 14(02): 206-216. **doi:** https://doi.org/10.20546/ijcmas.2025.1402.019